International Journal of Chemical, Materials and Biomolecular Sciences
ISSN: 2415-6620
Vol:11, No:2, 2017

Functionalization of Polypropylene with Chiral Monomer for Improving Hemocompatibility

Xiaodong Xu, Dan Zhao, Xiujuan Chang, Chunming Li, Huiyun Zhou, Xin Li, Qiang Shi, Shifang Luan, Jinghua Yin

***Abstract*—**Polypropylene (PP) is one of the most commonly used plastics because of its low density, outstanding mechanical properties, and low cost. However, its drawbacks such as low surface energy, poor dyeability, lack of chemical functionalities, and poor compatibility with polar polymers and inorganic materials, have restricted the application of PP. To expand its application in biomedical materials, functionalization is considered to be the most effective way. In this study, PP was functionalized with a chiral monomer, (*S*)-1-acryloylpyrrolidine-2-carboxylic acid ((*S*)-APCA), by free-radical grafting in the solid phase. The grafting degree of PP-g-APCA was determined by chemical titration method, and the chemical structure of functionalized PP was characterized by FTIR spectroscopy, which confirmed that the chiral monomer (*S*)-APCA was successfully grafted onto PP. Static water contact angle results suggested that the surface hydrophilicity of PP was significantly improved by solid phase grafting and assistance of surface water treatment. Protein adsorption and platelet adhesion results showed that hemocompatibility of PP was greatly improved by grafting the chiral monomer.

***Keywords*—**Functionalization, polypropylene, chiral monomer, hemocompatibility.

I. Introduction

PP is one of the most commonly used materials in medical apparatus and instruments, owing to its outstanding mechanical properties, non-toxic, and low cost. However, because of a lack of polar functional groups along the polymer backbone, neat PP exhibits poor biocompatibility, which limits its potential application in biomedical field. To expand its application, a lot of modification methods have been applied. Among these methods, graft copolymerization with polar monomers offers an effective approach to introduce polar functional groups on the inert PP backbone and thus introduce some desirable properties for PP.

Grafting of PP with polar monomers can be performed in solution, in the melt or in the solid state, whereas, in the latter, grafting modification is generally on the surface of membranes [1], [2]. Solid-phase grafting is a relatively new method developed in the early 1990s, which is performed below the melting point of PP powder [3], [4]. Compared with other grafting methods, solid-phase grafting has been attracted much attention because of its advantages such as lower reaction temperature, lower solvent requirement, and simpler reaction equipment. In addition, solid-phase grafting techniques assisted by supercritical carbon dioxide [1], [5]-[7], pan-milling [8], ball-milling [9], [10] or addition of comonomers [2], [11] have prepared graft copolymers with high grafting degree.

The most commonly used monomers for solid-phase grafting of PP are respectively maleic anhydride (MAH) [3], [4], [9]-[13], styrene (St) [14]-[16], glycidyl methacrylate (GMA) [1], [2], [17], methyl methacrylate (MMA) [18], [19]. Other monomers, such as acrylonitrile (AN) [18], butyl acrylate (BA) [5], [20], [21], butyl methylacrylate (BMA) [22], 4-vinyl pyridine (4-VP) [23], 2-hydroxyethyl methacrylate (2-HEMA) [6], have also been reported. However, chiral monomers have rarely been reported for the modification of PP. In this study, functionalization of PP with a chiral monomer containing amino acid residue, (*S*)-APCA, by solid-phase grafting was reported. The advantage of using chiral monomers with amino acid residues to modify polymers is that amino acid residues might modulate the bio-availability of polymers. Thus, the biocompatibility of polymers could be greatly improved.

II. Experimental

A. Materials

PP (P340) was supplied by Panjin Petrochemical Co., Panjin, China. It consists of ca. 5% ethylene content, a density of 0.91 g/cm^3 and MFR of 3.3 g/10 min (ASTM D-1238). Benzoyl peroxide (BPO, Tianjin Gugangfu fine Chemical Research Institute, China) was purified by recrystallization from methanol and stored in the refrigerator until use. Styrene (St, Tianjin Kermel Chemical Reagent Co., Ltd., China) was distilled under vacuum. L-Proline (Shanghai Jingchun Chemical Co., Ltd., China) and acryloyl chloride (Shanghai Hatch Chemical Co., Ltd., China) were used as received. The monomer (*S*)-APCA was synthesized by the reaction of acryloyl chloride with L-proline according to the procedures reported previously [24]. Other chemicals, such as xylene, acetone, methanol, ethanol, sodium hydroxide (NaOH), potassium hydroxide (KOH), N,N'-dimethylformamide (DMF), were all analytical reagent and used without further purification.

B. Grafting Procedure

The solid-phase grafting reaction was carried out according to the following procedure (Fig. 1). (*S*)-APCA was dissolved in

Xiaodong Xu is with Key Laboratory of Superlight Materials and Surface Technology, Ministry of Education, College of Materials Science and Chemical Engineering, Harbin Engineering University, Harbin 150001, China (corresponding author, phone: +86-451-82568191; fax: +86-451-82569890; e-mail: xuxiaodong@ hrbeu.edu.cn).

Qiang Shi is with State Key Laboratory of Polymer Physics and Chemistry, Changchun Institute of Applied Chemistry, Chinese Academy of Sciences, Changchun 130022, China (corresponding author, phone: +86-431-85262161; fax: +86-431-85262126; e-mail: shiqiang@ciac.ac.cn).

Jinghua Yin is with State key Laboratory of Polymer Physics and Chemistry, Changchun Institute of Applied Chemistry, Chinese Academy of Sciences, Changchun 130022, China (corresponding author, phone: +86-431-85262109; fax: +86-431-85262126; e-mail: yinjh@ciac.jl.cn).

DMF, St and BPO were dissolved in xylene. PP was placed in a two-necked flask equipped with a condenser tube and three-way stopcocks in a dry nitrogen atmosphere. (*S*)-APCA solution, St and BPO solution were introduced to the flask with syringes under nitrogen, then the flask was sealed. The mixture was stirred at room temperature for 1h for sufficient adsorption of the monomers and the initiator onto the PP particles, and the flask was placed in an oil bath at 110 °C for 30 min. The raw grafted PP was dissolved in xylene at 110 °C and precipitated in a large amount of methanol. The methanol-insoluble part, referred as PP-g-APCA/St, was extracted for 24h with acetone and methanol, respectively, and dried under vacuum at 60 °C.

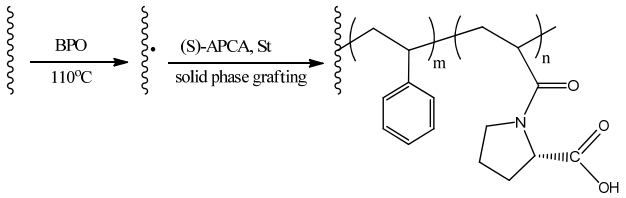

Fig. 1 Preparation of PP-g-APCA/St by solid phase grafting

C. Determination of Grafting Degree

The grafting degree of PP-g-APCA was determined by chemical titration method following the reference with a slight modification [25]. 0.2 g of purified PP-g-APCA was dissolved in 50 mL of xylene at 110 °C. After completely dissolved, 10 mL of 0.05 mol/L potassium hydroxide solution in ethanol was added into the flask, and the system was kept refluxing for 1h. The formed solution was back titrated with 0.05 mol/L (C_1) acetic acid solution in xylene (V_1). A blank test for PP was carried out by the same method. Grafting degree was calculated from the following equation:

$$G(\%\text{wt}) = \frac{C_1(V_0 - V_1)}{1000 \times m} \times M_{(S)\text{-APCA}} \times 100\% \quad (1)$$

where G(wt.%) is the grafting degree of PP-g-APCA, C_1 (mol/L) is the concentration of the acid solution, V_0 (mL) is the volume of the acid solution used in the blank test, V_1 (mL) is the volume of the acid solution used in the test with the sample, m (g) is the weight of the sample, and $M_{(S)\text{-APCA}}$=169.07 is the molecular weight of monomer (*S*)-APCA.

D.Spin Coated Film Preparation and Surface Restructuring

The xylene solutions of the grafted copolymers (0.5 wt.%) in the temperature range from 90 to 120 °C were spin-coated onto heated coverslip to form thin films. The thin films were then heated at 60 °C in a vacuum oven for 4h and immersed in distilled water at 60 °C for 24h. The treated films were finally dried in a vacuum oven at room temperature.

E. Characterization

Fourier transform infrared (FTIR) spectra of the hot-pressed films were measured by a PerkinElmer Spectrum 100 Series FTIR spectrometer. And the FTIR spectra of samples were recorded from 4000 to 450 cm^{-1} with a 4 cm^{-1} resolution.

FTIR microscopy images of PP-g-APCA/St were recorded on a PerkinElmer Spotlight 400 FTIR imaging system equipped with a liquid nitrogen cooled 16×1 pixel linear Mercury Cadmium Telluride (MCT) detector. The spectrum of air was used for the background subtraction. The FTIR spectra were collected with a 16 cm^{-1} resolution, a pixel size of 6.25 μm in the transmittance mode or 1.56 μm in the ATR mode, and 60 scans per pixel from 4000 to 650 cm^{-1}. The false color FTIR micrographs were processed from the chemical map of the integrated C=O stretching vibration of monomer (S)-APCA at 1730 cm^{-1}, 1650cm^{-1} and specific vibration of benzene ring of comonomer styrene at 699cm^{-1}, respectively.

The static water contact angles of the films were measured by the sessile drop method with a KRUSS GMBH DSA 100 drop shape analyzer at room temperature. For each sample, at least six measurements were performed.

For platelet adhesion test, 20 μL of fresh platelet-rich plasma was dropped onto the center of the spin-coated films (2 × 2 cm^2) and incubated for 2h at 37 °C. After incubation, the films were washed with PBS solution (pH 7.4) for three times to remove any non-adhered platelets, and the platelets adhered on the films were fixed by treatment with 2.5 wt.% glutaraldehyde in PBS at 4 °C for 10h. Finally, the films were washed with deionized water for three times and dehydrated with a series of ethanol/water mixtures (30, 50, 70, 90, and 100 vol.% ethanol for 30 min for each mixture). The films were then gold sputtered in vacuum and observed by a FEI XL 30 field emission scanning electron microscopy (FESEM) [26].

To evaluate the nonspecific protein adsorption resistance, the samples were first incubated in PBS solution for 2h, then soaked in PBS solution containing FITC-labeled fibrinogen or RBITC-labeled BSA (200 μg/mL) at 4 °C for 12h, rinsed and dried. The fluorescence intensity scanning was carried out by a confocal laser scanning microscope (Zeiss, LSM 700). The samples labeled with FITC and RBITC were exposed to an excitation source of argon ion laser at 488 nm and 555 nm, respectively. In order to obtain fluorescence intensity, original fluorescent images were analyzed using Image-Pro software. Fluorescence intensity value was measured from six different positions of each fluorescence image.

III. Results and Discussion

A. FTIR Spectrum of PP-g-APCA/St

FTIR spectra of PP and PP-g-APCA/St are shown in Fig. 2. The strong absorption band from 2980 cm^{-1} to 2830 cm^{-1} is attributed to the stretching vibration of C-H bond in the PP molecular chain, while those at 1456 cm^{-1} and 1376 cm^{-1} is assigned to the bending vibration of C-H bond in the PP molecular chain. Compared with the spectrum of PP, three new absorption bands at 1730 cm^{-1}, 1650 cm^{-1}, and 699 cm^{-1}, respectively, appear in the spectrum of PP-g-APCA/St. The former two bands are attributed to the carbonyl group of carboxyl group and tertiary amido group in the grafting monomer (S)-APCA, while the latter band at 699 cm^{-1} is assigned to the benzene ring in the comonomer styrene. These features indicate that (S)-APCA and St are successfully grafted on the molecular chains of PP.

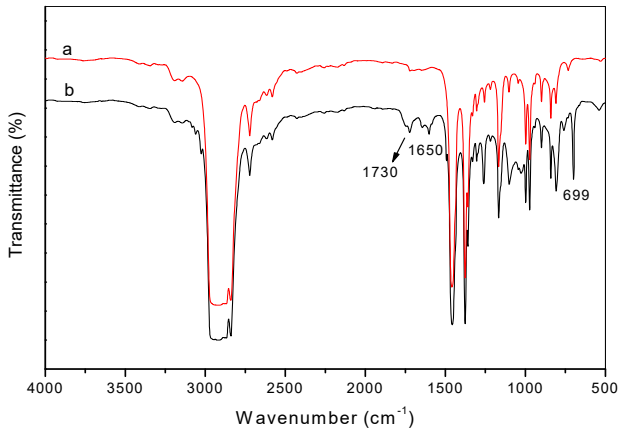

Fig. 2 FTIR spectra of PP (a) and PP-g-APCA/St (b) (grafting degree of APCA = 5.1%)

B. Distribution of Functional Groups in PP-g-APCA/St

For grafted PP, conventional FTIR spectrum can only provide the information of chemical composition. FTIR microscopy imaging, on the other hand, allows the possibility to further visualize the distribution of functional groups. The false color FTIR micrographs of PP and PP-g-APCA/St obtained in the transmittance mode are shown in Fig. 3. The false color code represents the signal intensity of the corresponding vibration when the intensity scales range from dark blue (low intensity) to pink (high intensity). Figs. 3 (b_1) and 2 (b_2) reveal the chemical map of the integrated C=O stretching vibration of monomer (S)-APCA in PP-g-APCA/St at 1730 cm^{-1} and 1650 cm^{-1}, respectively. It can be seen that the two groups are well distributed in PP-g-APCA/St, which indicates an even distribution of APCA segments in PP-g-APCA/St. Fig. 3 (b_3) represents the integrated specific vibration of benzene ring of comonomer styrene in PP-g-APCA/St at 699 cm^{-1}, which shows a well-distribution of styrene segments in PP-g-APCA/St. Conversely, the very low intensity of the above three vibration bands indicates that there are nearly no functional groups in the neat PP, as shown in Figs. 3 (a_1), (a_2), and (a_3).

C. Surface Properties of PP-g-APCA/St Film

To evaluate the surface hydrophilicity of the PP films, the static water contact angle of the neat PP and grafted PP on the surfaces of the spin-coated films was measured, and the results are shown in Fig. 4. The static water contact angle of the neat PP film is 130.8°. After solid-phase grafting with (S)-APCA, the static contact angle significantly decreased to 112.0°. Nevertheless, the surface of grafted PP film is still hydrophobic. On the other hand, after the film of the grafted PP was immersed in water at 60 °C for 24h, the static contact angle decreased correspondingly from 112.0° to 86.5°. This indicated that surface rearrangement occurred, and more (S)-APCA segments were induced to enrich on the topmost layer of the surface by the interaction with water [27].

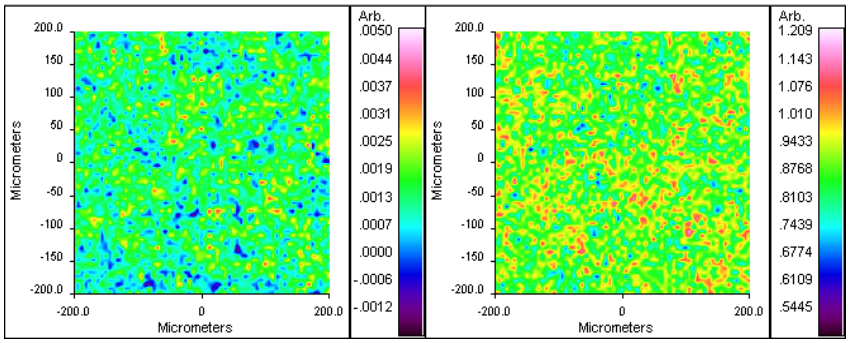

(a_1) (b_1)

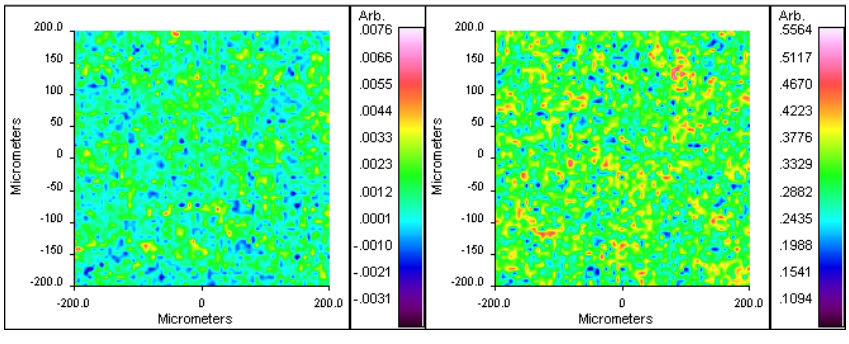

(a_2) (b_2)

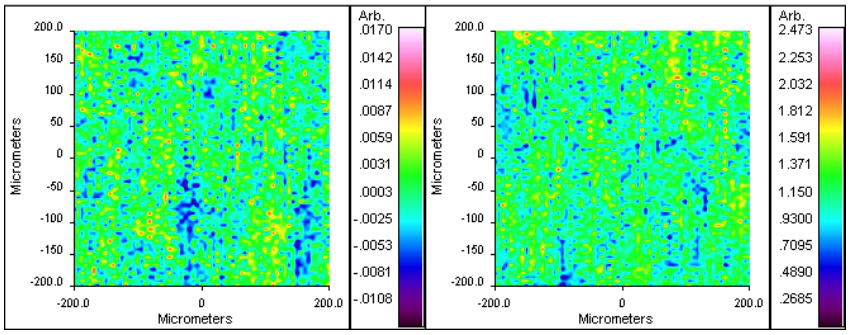

(a_3) (b_3)

Fig. 3 False color FTIR micrographs of PP (a) and PP-g-APCA/St (b) (grafting degree of APCA = 5.1%) from the chemical map of the integrated vibration at (1) 1730 cm^{-1}, (2) 1650 $cm^{-1}$and (3) 699 cm^{-1}

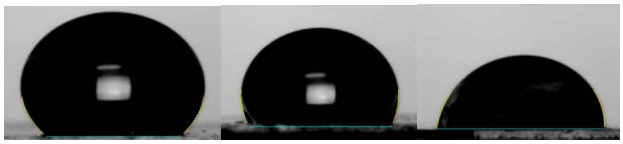

(a) 130.8±2.2° (b) 112.0±2.6° (c) 86.5±4.6°

Fig. 4 Water contact angle values on the surfaces of neat PP (a), PP-g-APCA/St (GD_{APCA} = 5.1%) before (b) and after (c) surface restructuring

To confirm the enrichment of (S)-APCA segments on the surface of the grafted PP films, FTIR micrographs before and after surface restructuring were obtained in ATR mode and are shown in Fig. 5. Figs. 5 (a_1) and (a_2) reveal the chemical map of the integrated C=O stretching vibration of monomer (S)-APCA before surface restructuring at 1730 cm^{-1} and 1650 cm^{-1}, respectively. While Figs. 5 (b_1) and 4(b_2) reveal the chemical map of the integrated C=O stretching vibration of monomer (S)-APCA after surface restructuring at 1730 cm^{-1} and 1650 cm^{-1}, respectively. Comparing Fig. 5 (b_1) with Fig. 4 (a_1), the intensity of absorption band at 1730 cm^{-1} for the surface restructuring sample is over two times more than that of the sample without surface restructuring. And same results can be observed from the comparison of Fig. 5 (b_2) with (a_2) for the absorption band at 1650 cm^{-1}. These results suggest that C=O groups, represented the (S)-APCA segments, are induced to enrich on the surface of the grafted PP film by the surface restructuring.

D. Protein Adhesion

It has been reported that when a foreign surface contacts blood, the initial response is protein adsorption on the surface, followed by platelet adhesion and activation of coagulation pathways, which lead to thrombus formation [28]. Therefore, protein adsorption on the film surfaces is essential to evaluate the hemocompatibility of the biomaterials. Herein, fibrinogen and BSA were used as model proteins. The protein adsorption on the surfaces of the neat PP and PP-g-APCA/St films with and without surface restructuring is shown in Fig. 6.

As shown in Fig. 6 (a_1), the neat PP film was found to exhibit the highest fibrinogen adsorption because of its hydrophobicity. Decreased fibrinogen adsorption was observed on the PP-g-APCA/St film without surface restructuring (Fig. 6 (b_1)). Further fibrinogen adsorption decrease was observed on the PP-g-APCA/St film after surface restructuring (Fig. 6 (c_1)). These results demonstrate that the graft copolymers with restructured surfaces (enrichment of (S)-APCA segments on the topmost layer) possessed high biocompatibility. Fig. 7 shows the corresponding normalized fluorescence intensity of the neat PP and PP-g-APCA/St films with and without surface restructuring. Adsorption of FITC-labeled fibrinogen decreased 75% and 43% for the PP-g-APCA/St films with and without surface restructuring, respectively. While adsorption of RBITC-labeled BSA decreased 73% and 62% for the corresponding films.

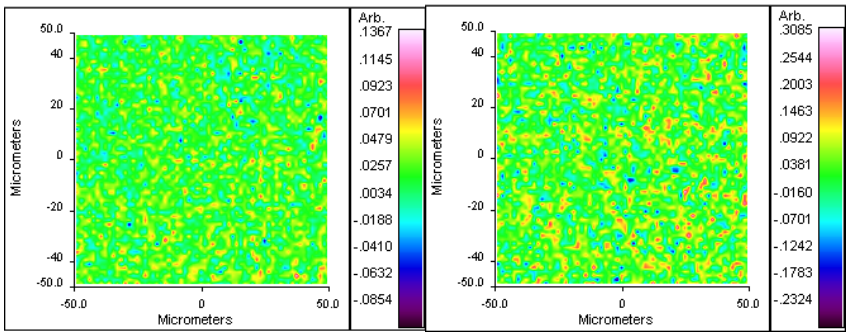

(a_1) (b_1)

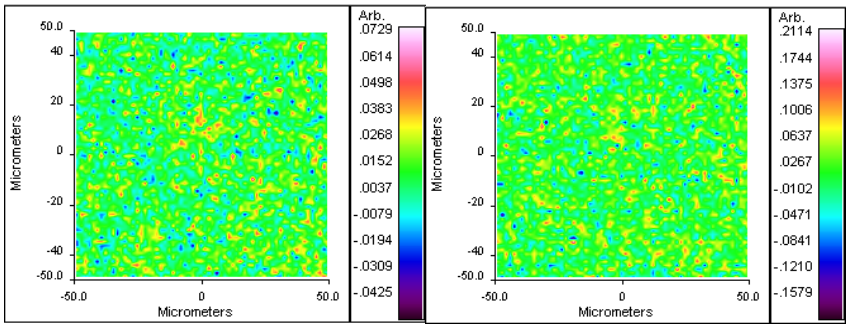

(a_2) (b_2)

Fig. 5 False color FTIR micrographs of PP-g-APCA/St (grafting degree of APCA = 5.1%) from the chemical map of the integrated vibration at (1) 1730 cm^{-1} and (2) 1650 cm^{-1} before (a) and after (b) surface restructuring

E. Platelet Adhesion

SEM micrographs of the platelets adhesion on the neat PP and PP-g-APCA/St films before and after surface restructuring are shown in Fig. 8. For the neat PP film (Fig. 8 (a)), a rough surface with superhydrophobic structure was observed. After contacting with platelet-rich plasma, almost no platelets adhered on the surface of neat PP film (Fig. 8 (b)). For PP-g-APCA/St film without surface restructuring, a great number of platelets were attached to the surface, and most of them showed extended pseudopodia (Fig. 8 (c)). For PP-g-APCA/St film after surface restructuring, nonactivated platelets adhesion was rarely observed (Figs. 8 (d) and (e)). But, a high number of small particles were observed on the surface of PP-g-APCA/St film after surface restructuring. By comparing with the control sample of PP-g-APCA/St film (Fig. 8 (f)), the small particles may come from the domains rich in (S)-APCA chains. The overall results provide evidence that the restructured surfaces of the functionalized PP enriched in (S)-APCA chains possessed high biocompatibility.

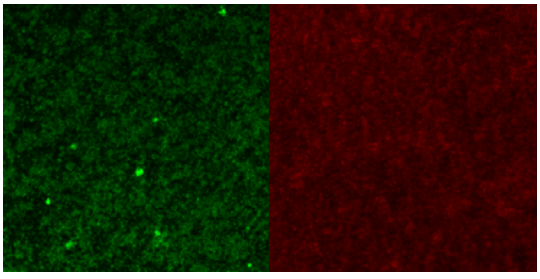

(a_1) (a_2)

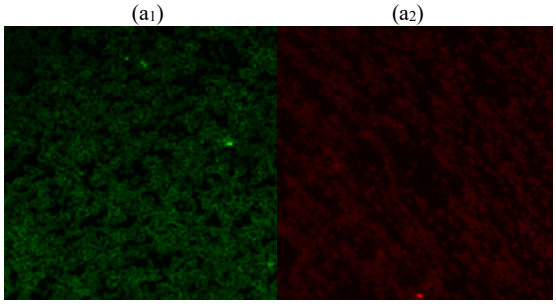

(b_1) (b_2)

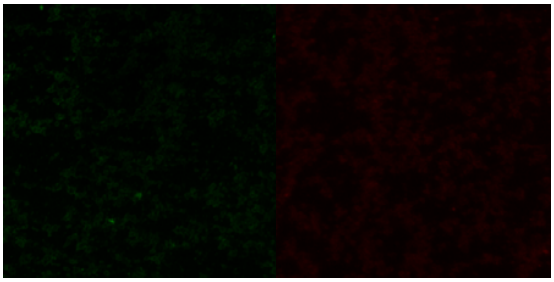

(c_1) (c_2)

Fig. 6 Confocal laser scanning micrographs of FITC-labeled fibrinogen (1) and RBITC-labeled BSA (2) adsorption on the surfaces of (a) neat PP, (b) PP-g-APCA/St without surface restructuring and (c) PP-g-APCA/St with surface restructuring

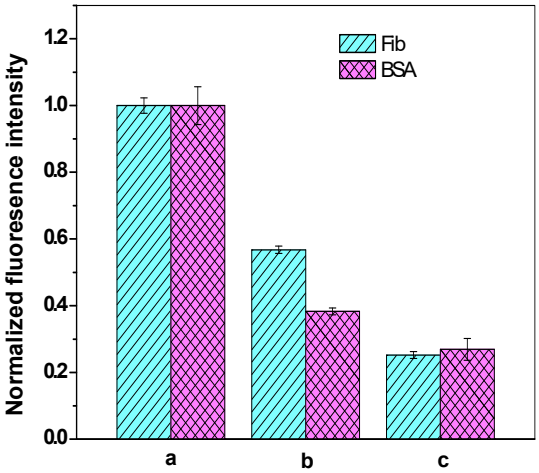

Fig. 7 Adsorption of FITC-labeled fibrinogen and RBITC- labeled BSA on the surfaces of (a) neat PP (b) PP-g-APCA/St without surface restructuring, (c) PP-g-APCA/St with surface restructuring

IV. Conclusions

Chiral monomer (S)-APCA was successfully grafted onto PP in the solid phase, which was confirmed by FTIR spectroscopy. FTIR micrographs indicated a homogeneous distribution of the functional groups in the modified PP. After solid phase

grafting, the surface hydrophilicity of PP was significantly improved by the assistance of surface water treatment. Chiral monomer modified PP shows a potential application in hemocompatible materials.

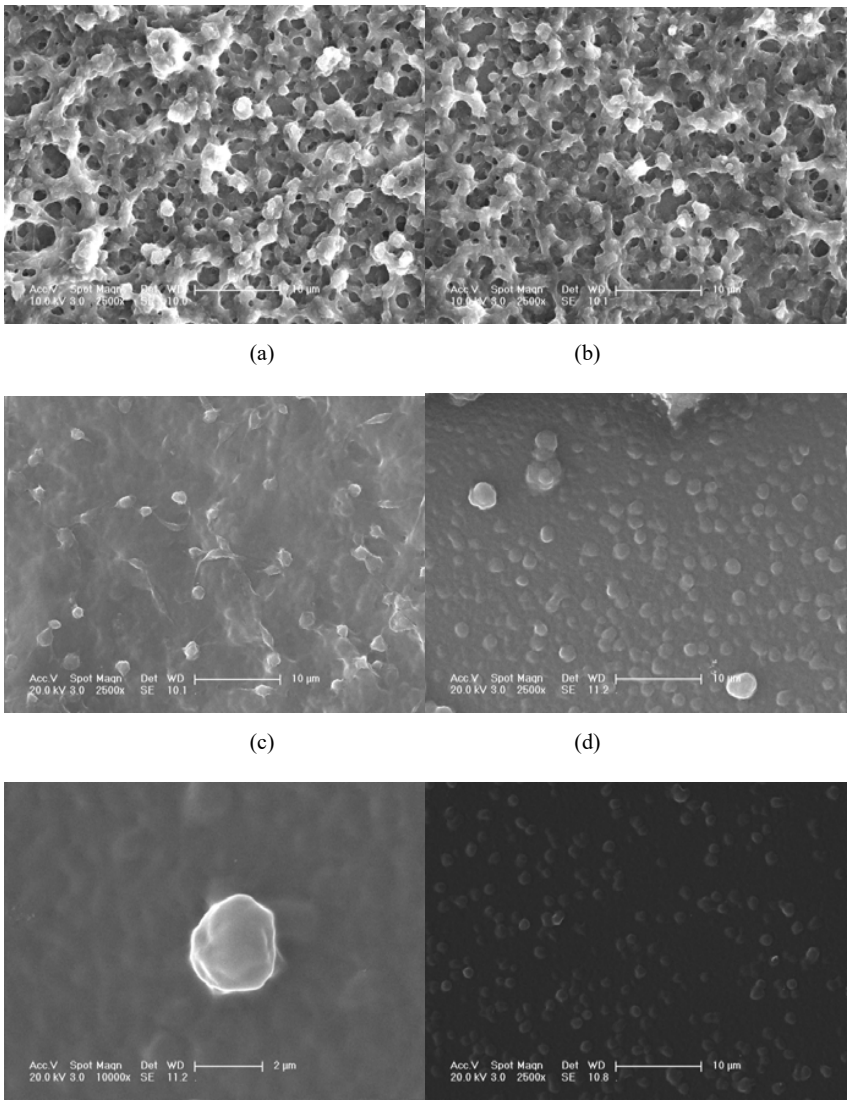

Fig. 8 SEM micrographs of the neat PP film (a), platelet adhesion on the surfaces of the neat PP (b), PP-g-APCA/St film without surface restructuring (c), PP-g-APCA/St film with surface restructuring (d) and (e), and control sample of PP-g-APCA/St film with surface restructuring

ACKNOWLEDGMENT

This work was financially supported by the National Natural Science Foundation of China (No. 51473167), the Natural Science Foundation of Heilongjiang Province of China (No. E201419), the Harbin City Scientific and Technological Innovation Fund of China (No. 2013RFLXJ027), the Open Research Fund of State Key Laboratory of Polymer Physics and Chemistry, Changchun Institute of Applied Chemistry, Chinese Academy of Sciences, and Harbin Engineering University.

REFERENCES

[1] M. H. Kunita, A. W. Rinaldi, E. M. Girotto, E. Radovanovic, E. C. Muniz, A. F. Rubira, "Grafting of glycidyl methacrylate onto polypropylene using supercritical carbon dioxide," *Eur. Polym. J.,* vol. 41, pp. 2176–2182, September 2005.

[2] D. M. Jia, Y. F. Luo, Y. M. Li, H. Lu, W. W. Fu, W. L. Cheung, "Synthesis and characterization of solid-phase graft copolymer of polypropylene with styrene and maleic anhydride," *J. Appl. Polym. Sci.,* vol. 78, pp. 2482–2487, December 2000.

[3] R. Rengarajan, M. Vicic, S. Lee, "Solid phase graft copolymerization: 2. Effect of toluene," Polymer, vol. 30, pp. 933–935, May 1989.

[4] S. Lee, R. Rengarajan, V. R. Parameswaran, "Solid phase graft copolymerization: Effect of interfacial agent," *J. Appl. Polym. Sci.*, vol. 41, pp. 1891–1894, December 1990.

[5] J. Wang, D. F. Wang, W. Du, E. G. Zou, Q. Dong, "Supercritical carbon dioxide-assisted solid-phase free radical grafting of butyl acrylate onto PP," *e-Polymers,* No. 097, pp. 1–15, August 2009.
[6] D. Li, B. X. Han, Z. M. Liu, "Grafting of 2-Hydroxyethyl Methacrylate onto Isotactic Poly(propylene) Using Supercritical CO2 as a Solvent and Swelling Agent," *Macromol. Chem. Phys.,* vol. 202, pp. 2187–2194, July 2001.
[7] Q. Z. Dong, Y. Liu, "Styrene-Assisted Free-Radical Graft Copolymerization of Maleic Anhydride onto Polypropylene in Supercritical Carbon Dioxide," *J. Appl. Polym. Sci.,* vol. 90, pp. 853–860, October 2003.
[8] C. S. Liu, Q. Wang, "Solid-Phase Grafting of Hydroxymethyl Acrylamide onto Polypropylene through Pan Milling," *J. Appl. Polym. Sci.,* vol. 78, pp. 2191–2197, December 2000.
[9] W. L. Qiu, T. Endo, T. Hirotsu, "A novel technique for preparing of maleic anhydride grafted polyolefins," *Eur. Polym. J.,* vol. 41, pp. 1979–1984, September 2005.
[10] W. L. Qiu, T. Hirotsu, "A New Method to Prepare Maleic Anhydride Grafted Poly(propylene)," *Macromol. Chem. Phys.,* vol. 206, pp. 2470–2482, December 2005.
[11] L. F. Zhang, B. H. Guo, Z. M. Zhang, "Synthesis of Multifunctional Polypropylene via Solid Phase Cografting and Its Grafting Mechanism," *J. Appl. Polym. Sci.,* vol. 84, pp. 929–935, May 2002.
[12] R. Rengarajan, V. R. Parameswaran, S. Lee, M. Vicic, P. L. Rinaldi, "N.m.r. analysis of polypropylene-maleic anhydride copolymer," *Polymer,* vol. 31, pp. 1703–1706, September1990.
[13] C. Ding, H. He, B. C. Guo, D. M. Jia, "Structure and Properties of Polypropylene/Clay Nanocomposites Compatibilized by Solid-Phase Grafted Polypropylene," *Polym. Compos.,* vol. 29, pp. 698–707, June 2008.
[14] F. Picchioni, J. G. P. Goossens, M. van Duin, "Solid-State Modification of Isotactic Polypropylene (iPP) via Grafting of Styrene. II. Morphology and Melt Processing," *J. Appl. Polym. Sci.,* vol. 97, pp. 575–583, July 2005.
[15] Q. T. Deng, Z. S. Fu, F. L. Sun, J. T. Xu, Z. Q. Fan, "Influence of an Annealing Treatment on the Solid-State Grafting of Styrene onto Spherical Isotactic Polypropylene Granules," *J. Appl. Polym. Sci.,* vol. 110, pp. 1990–1996, November 2008.
[16] F. L. Sun, Z. S. Fu, Q. T. Deng, Z. Q. Fan, "Solid-State Graft Polymerization of Styrene in Spherical Polypropylene Granules in the Presence of TEMPO," *J. Appl. Polym. Sci.,* vol. 112, pp. 275–282, April 2009.
[17] Y. K. Pan, J. M. Ruan, D. F. Zhou, "Solid-Phase Grafting of Glycidyl Methacrylate onto Polypropylene," *J. Appl. Polym. Sci.,* vol. 65, pp. 1905–1912, September 1997.
[18] A. C. Patel, R. B. Brahmbhatt, P. V. C. Rao, S.Devi, "Solid phase grafting of various monomers on hydroperoxidized polypropylene," *Eur. Polym. J.,* vol. 36, pp. 2477–2484, November 2000.
[19] H. L. Peng, Y. F. Luo, H. Q. Hong, L. Liu, D. M. Jia, "Study on Crystallization Behavior of Solid-Phase Graft Copolymers of Polypropylene with Maleic Anhydride and Methyl Methacrylate," *Polym. Plast. Technol. Eng.,* vol. 47, pp. 996–1001, October 2008.
[20] H. Q. Hong, D. M. Jia, H. He, "Influences of Grafted Side Chains on the Viscoelastic Behavior of Ternary Graft Copolymers," *Polym. Plast. Technol.Eng.,* vol. 45, pp. 1263–1269, November 2006.
[21] H. Q. Hong, H. He, D. M. Jia, C. Ding, F. Xue, Y. P. Huang, "Influences of Ternary Graft Copolymers on the Morphology and Properties of Polypropylene/Calcium Carbonate Composites," *Polym. Plast. Technol. Eng.,* vol. 45, pp. 379–387, March 2006.
[22] J. Wang, D. F. Wang, W. Du, E. G. Zou, Q. Dong, "Synthesis of Functional Polypropylene Via Solid-Phase Grafting Soft Vinyl Monomer and Its Mechanism," *J. Appl. Polym. Sci.,* vol. 113, pp. 1803–1810, August 2009.
[23] R. B. Brahmbhatt, A. C. Patel, R. C. Jain, S. Devi, "Solid phase grafting of 4-vinylpyridine onto isotactic polypropylene," *Eur. Polym. J.,* vol. 35, pp. 1695–1701, September 1999.
[24] G. L. Zhang, L. L. Chen, L. L. Qiu, X. D. Xu, J. Feng, "Preparation and Characterization of Poly(Acrylonitrile-co-1-Acryloylpyrrolidine-2-Carboxylic Acid) with High Molecular Weight,"*J. Macromol. Sci., Part B: Phys.*, vol. 52, pp. 1298–1308, September 2013.
[25] D. Shi, J. H. Yang, Z. H. Yao, Y. Wang, H. L. Huang, J. Wu, J. H. Yin, G. Costa, "Functionalization of isotactic polypropylene with maleic anhydride by reactive extrusion: mechanism of melt grafting," *Polymer,* vol. 42, pp. 5549–5557, June 2001.
[26] J. Jin, W. Jiang, Q. shi, J. Zhao, J. H. Yin, P. Stagnaro, "Fabrication of PP-g-PEGMA-g-heparin and its hemocompatibility: From protein adsorption to anticoagulant tendency," *Appl. Surf. Sci.,* vol. 258, pp. 5841–5849, May 2012.
[27] Q. Shi, J. Zhao, P. Stagnaro, H. Yang, S. F. Luan, J. H. Yin, "Biocompatible Polypropylene Prepared by a Combination of Melt Grafting and Surface Restructuring," *J. Appl. Polym. Sci.,* vol. 126, pp. 929–938, November 2012.
[28] H. Cheng, L. Yuan, W. Song, Z. Wu, D. Li. "Biocompatible polymer materials: Role of protein-surface interactions," *Prog. Polym. Sci*., vol. 33, pp. 1059–1087, November 2008.